MOLECULAR ONCOLOGY 4 (2010) 529–538

available at www.sciencedirect.com

ScienceDirect

www.elsevier.com/locate/molonc

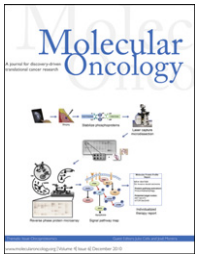

Review

MALDI Imaging Mass Spectrometry – Painting Molecular Pictures

*Kristina Schwamborn, Richard M. Caprioli**

Mass Spectrometry Research Center and the Department of Biochemistry, Vanderbilt University, Nashville, TN, USA

ARTICLE INFO

Article history:
Received 9 June 2010
Received in revised form
20 September 2010
Accepted 20 September 2010
Available online 25 September 2010

Keywords:
Imaging Mass Spectrometry
Proteomics
Cancer

ABSTRACT

MALDI Imaging Mass Spectrometry is a molecular analytical technology capable of simultaneously measuring multiple analytes directly from intact tissue sections. Histological features within the sample can be correlated with molecular species without the need for target-specific reagents such as antibodies. Several studies have demonstrated the strength of the technology for uncovering new markers that correlate with disease severity as well as prognosis and therapeutic response. This review describes technological aspects of imaging mass spectrometry together with applications in cancer research.

1. Introduction

The study of proteins and their role in health and disease fully encompasses basic research and clinical studies (Krieg et al., 2002). As the proteome is more complex and dynamic than the genome, it holds the prospect of providing exciting new approaches for the identification of molecular markers (Celis and Gromov, 2003). Proteomic studies utilize several platform technologies that allow high throughput and high sensitivity investigations, e.g., mass spectrometry (MS), reverse phase protein microarrays (as discussed in detail in this issue by (Mueller et al., 2010)) and 2D gel electrophoresis. MS has proven to be a versatile and powerful tool for the analysis of proteins and peptides as well as other biological compounds such as DNA segments, lipids, metabolites, as well as other small molecules (van der Merwe et al., 2007). In particular, matrix assisted laser desorption/ionization (MALDI) MS is a state-of-the-art technology for analyzing protein profiles in clinical samples as advances in mass spectrometry instrumentation and bioinformatics have been achieved to meet the challenge of complexity inherit to biological samples (Chen and Yates, 2007).

2. MALDI mass spectrometry

The versatility of MS as an analytical tool in various areas of research including studies of drug metabolism, lipidomics (Schiller et al., 2004), genomics (Harvey et al., 1995; Tost and Gut, 2006) and proteomics (Aebersold and Mann, 2003) has made the technology a centerpiece in many laboratories. With the introduction of MALDI MS, the analysis of intact proteins could be achieved (Karas and Hillenkamp, 1988; Tanaka et al., 1988) with high sensitivity and high mass accuracy (Aebersold and Mann, 2003). Briefly, samples are prepared by mixing or coating with a solution of an energy absorbant matrix, typically a small organic compound that crystallizes on drying. Desorption and ionization are achieved by irradiating

* *Corresponding author.*
E-mail address: richard.m.caprioli@Vanderbilt.Edu (R.M. Caprioli).
1574-7891/$ – see front matter © 2010 Federation of European Biochemical Societies. Published by Elsevier B.V. All rights reserved.
doi:10.1016/j.molonc.2010.09.002

the sample with a laser beam, commonly generating singly protonated ions from analytes in the sample. Measurement and detection of the charged analytes can be performed with several different types of mass analyzers, although time of flight (TOF) analyzers are often used. Following acceleration at a fixed potential, ions are separated and recorded as a consequence of their mass-to-charge ratio (m/z). Figure 1 shows the schematic outline of a typical MALDI TOF mass spectrometer.

3. MALDI Imaging Mass Spectrometry

One emerging and promising new technology for protein analysis from intact biological tissues is MALDI Imaging Mass Spectrometry (IMS), introduced in 1997 (Caprioli et al., 1997). This technology allows for direct mass spectrometric analysis of tissue sections. The relative abundance and spatial distribution of proteins and peptides throughout a tissue section can be visualized with a lateral resolution of up to 10 μm using current instrumentation (Chaurand et al., 2004; Seeley and Caprioli, 2008). This technology makes use of MALDI and requires the section to be coated with a matrix solution (Cornett et al., 2007), either by spray coating or by use of a robotic matrix spotter (Chaurand et al., 2005). Mass spectrometric data is acquired by performing a raster of the sample by the laser beam utilizing a grid pattern with a predefined number of laser shots per grid coordinate (Seeley and Caprioli, 2008). IMS can also be applied to formalin-fixed and paraffin-embedded (FFPE) tissues, an important aspect since the vast majority of tissue with correlating clinical follow up data are collected and stored by pathologists as FFPE samples. Until recently, FFPE samples were believed to be unusable for proteomic approaches due to protein cross-linking caused by formalin fixation (Becker et al., 2007). However, use of antigen retrieval techniques coupled with *in situ* tryptic digestion has allowed the analysis of FFPE samples by IMS (Groseclose et al., 2008).

Current classical protocols require cells of interest to be collected from the surrounding tissue compartments to help enrich for specific cell populations due to the heterogeneity of most tissue samples. This is necessary to prevent a contamination by other cells that, even when in minority, might significantly contribute to a measurement. Microdissecting techniques (e.g., laser capture microdissection, LCM) are well established but tedious (Krieg et al., 2005). In addition, the minimal requirement of protein content for MS analysis is often difficult to obtain, especially if cells of interest are small in number.

IMS directly analyzes complex biological samples such as tissues, combining the positive features of immunohistochemistry (IHC) in being able to measure the distribution of molecules within a sample and the molecular specificity of MS. Moreover, IMS allows an unbiased approach for molecular discovery because it does not require target-specific labeling reagents such as antibodies. Since it utilizes intact tissue, IMS enables the correlation of molecular information with histological details, unlike other MS based proteomic technologies that require tissue homogenization, thereby losing spatial information/histology of the tissue.

IMS experiments can generally be performed in two related modes, imaging (Stoeckli et al., 2001) and profiling (Cornett et al., 2006). Profiling represents a targeted analysis approach whereby small areas of interest are individually analyzed that have been selected prior to MS analysis. For example, groups of cells (e.g., cancer and normal) can be identified on a serial section and these can be selectively analyzed. Profiling is typically used in studies analyzing heterogeneous tissues where only a selected cell population or selected areas of the tissue are of prime interest. Imaging experiments, on the other hand, measure the overall distribution of analytes throughout the entire tissue section or specified region of interest. Ion distribution maps of each signal in the mass spectra can be displayed and correlated with histological features. Imaging and profiling are complementary in that sections may be imaged at high resolution following initial molecular discovery from a profiling experiment. A typical workflow of an imaging experiment is outlined in Figure 2.

Sample preparation protocols are similar for both imaging and profiling. For fresh frozen tissue samples, 5–20 μm thick sections are cut on a cryostat and thaw mounted on a metal target or conductive glass slide. For protein analysis, excess lipids and salts can interfere with matrix crystallization and analyte ionization, therefore sections are typically fixed with graded ethanol washes (70%, 90%, 95% for 30 s each). This established histology procedure also ensures sample dehydration and fixation of the proteins while maintaining the tissue architecture. Some histological stains such as hematoxylin and eosin (H&E) interfere with subsequent MS analyses, thus serial sections are often obtained and stained to guide matrix deposition and laser ablation (i.e., in a histology-directed profiling experiment) and to allow comparison of MS results with tissue histology. Some simple stains such as cresyl violet or

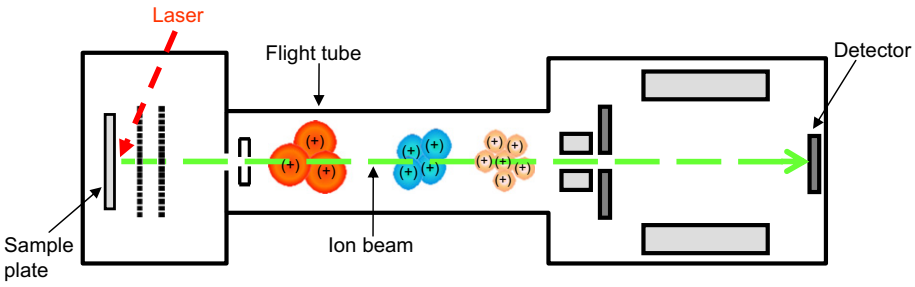

Figure 1 – Schematic outline of a typical linear time of flight mass spectrometer. Analyte ions are separated based on their mass-to-charge ratio (m/z).

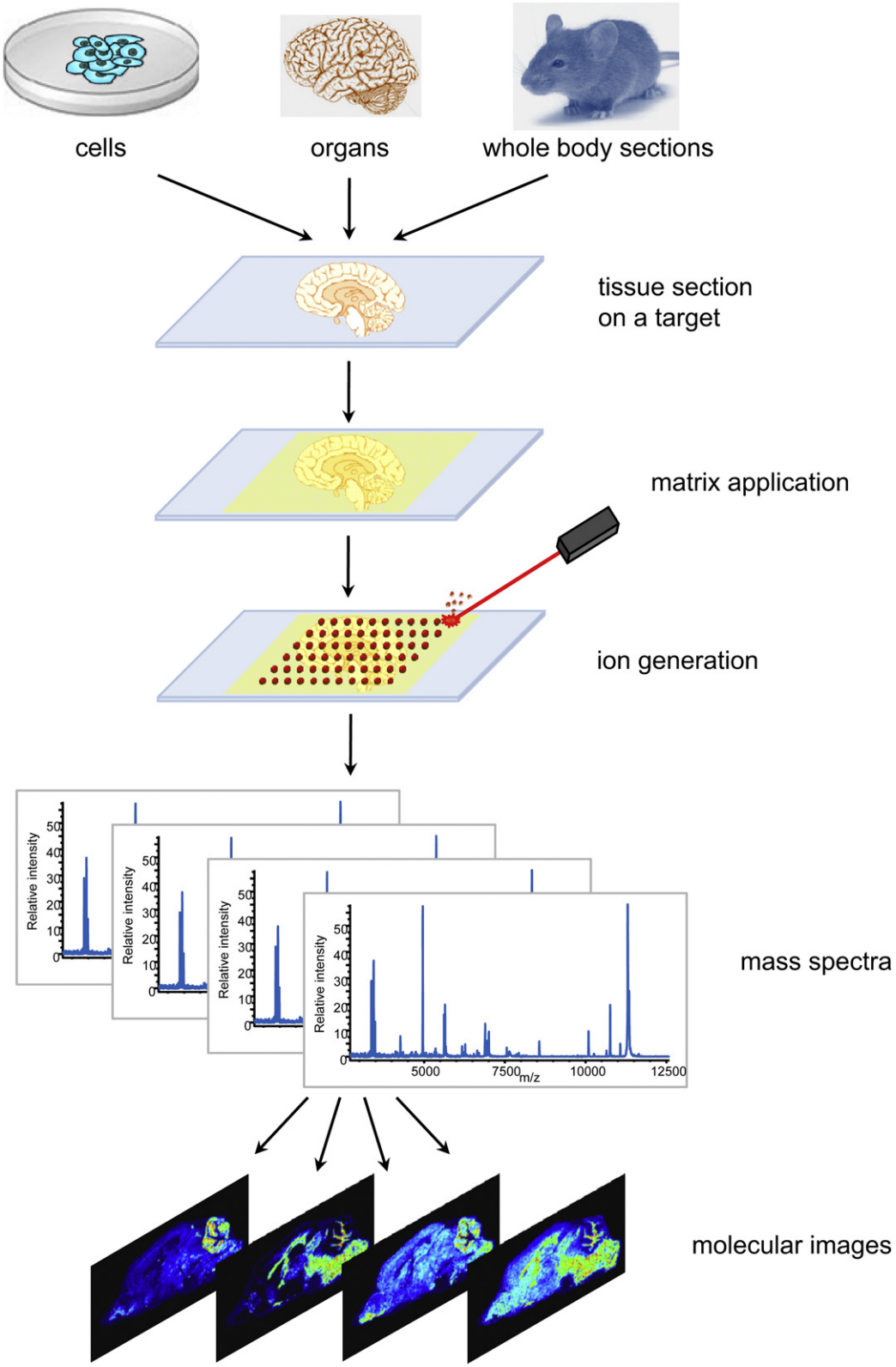

Figure 2 – Schematic outline of a typical workflow for an IMS experiment. Sample pretreatment steps include cutting, mounting the sample on a target and matrix application. Mass spectra are generated in an ordered array at each *x*, *y* coordinate. Individual spectral features can be visualized within the tissue to generate protein images.

methylene blue are compatible with subsequent MS analysis and can be used on the same section (Chaurand et al., 2004). An alternative procedure that allows H&E staining of the same section involves first performing MS analysis followed by matrix removal and subsequent staining. Several classes of proteins such as integral membrane proteins or hydrophobic proteins are usually under-represented due to inherent difficulties in solubility. In this case, special sample pretreatment protocols are employed to deplete tissue sections of abundant soluble proteins (Grey et al., 2009).

Application of matrix in a MALDI MS experiment is a critical step of the sample preparation process (Schwartz et al., 2003) and has to be performed in a manner that allows optimal analyte extraction from the tissue and sufficient matrix crystal formation while avoiding analyte migration. The latter is of special importance since typical MALDI matrices for protein analysis are applied to tissues in solution. In the case of imaging and profiling of lipids, alternative matrix application strategies can be used including dry coating (Puolitaival et al., 2008) and sublimation (Hankin et al., 2007). The choice of matrix depends on the analytes to be analyzed; for protein analysis (molecular weight $>$ 2 kDa) the matrix of choice is sinapinic acid (SA), for peptides (molecular weight 500–3000 Da) α-cyano-4-hydroxycinnamic acid (CHCA), and for small molecules such as lipids and drugs, 2,5-dihydroxybenzoic acid (DHB). The matrix is typically dissolved in a solvent solution containing 50% acetonitrile with 0.1% trifluoroacetic acid (Herring et al., 2007). Although manual application of ~250 nL–1 μL matrix solution in general produces high quality mass spectra, this results in relatively large matrix spots (0.5–1 mm in diameter) and therefore, is not recommended for most studies that require medium to high spatial resolution. Profiling experiments are best performed by accurate placement of small matrix spots through the use of robotic spotting devices (Aerni et al., 2006; Sloane et al., 2002). These instruments are capable of depositing 50–100 pL volumes at specific x, y coordinates on tissue sections. Multiple passes of matrix application may be required to achieve optimal analyte extraction and matrix crystallization. Commercial robotic instruments typically produce matrix spots on tissue of 100–180 μm in diameter. Matrix application for imaging experiments is performed by either applying the matrix in an ordered array of dense matrix spots using robotic devices or by spraying the matrix onto the tissue to achieve a homogeneous coating. The latter can be obtained manually, e.g., using a thin layer chromatography sprayer (Schwamborn et al., 2007; Schwartz et al., 2003), or by utilizing instruments that form a thin layer of small matrix crystals on the surface of the tissue section (Kruse and Sweedler, 2003; Walch et al., 2008). Care must be taken to wet the tissue section to achieve an efficient analyte extraction while avoiding analyte delocalization. Typically, multiple cycles of light spraying and drying are performed to achieve optimal matrix application.

FFPE tissue samples require special sample preparation steps prior to matrix application. Samples are typically cut at 5 μm using a microtome and mounted onto conductive targets. After paraffin removal in xylene and graded ethanol washes, in accordance with established immunohistochemistry protocols, sections are antigen retrieved, typically by incubating the section in a heated buffer solution (e.g., citrate or tris buffer) for 20 min. Subsequently, on-tissue enzymatic digestion is performed, usually by robotically spotting enzyme solution on the tissue in the same manner as that described above for matrix application (Groseclose et al., 2008; Ronci et al., 2008). Following digestion, matrix is applied to these spots; and the tissue is analyzed.

Data is acquired for both profiling and imaging similarly by moving the sample stage under a fixed laser focus position. At each x, y position, multiple laser shots are summed to generate a single spectrum for that given position. For protein analyses, mass spectra are typically acquired in a mass range from 2 to 50 kDa. Although higher molecular weight proteins (e.g., over 200 kDa) can be measured from tissue sections (Chaurand and Caprioli, 2002; Chaurand et al., 2002); instrument-tuning parameters must be optimized for this application.

Mass spectral processing steps include baseline subtraction, noise reduction, mass calibration and normalization to total ion current (TIC) of each spectrum. Features of interest, detected peak areas or intensities that meet certain threshold criteria (ie, minimal S/N, prevalence in certain percentage of sampled spectra) can be subjected to statistical analysis. For example, spectra from each sample group analyzed can be compared to determine features that are significantly different between the groups. Specific algorithms, many of which were initially developed for genomic data analysis, are capable of combining multiple spectral features in a model that can distinguish between spectra from each group. In imaging experiments, software tools enable the identification of signals that are unique to specific features within the tissue sample. The adoption of unsupervised as well as supervised classification algorithms facilitates data analysis to generate digital stained images of tissue (Deininger et al., 2008; Hanselmann et al., 2009). Generation of reconstructed three-dimensional (3D) volumes also can be achieved utilizing virtual z-stacks and 3D volume rendering tools. IMS based data can be co-registered with additional data such as block face optical images and MRI data (Andersson et al., 2008; Crecelius et al., 2005; Sinha et al., 2008), as shown in Figure 3.

4. Applications

The use of IMS in cancer research primarily comprises studies of proteins and peptides, although there is an increased interest in the investigation of the distribution of differentially expressed lipid species as well as drug distribution in tissue sections. This review will mainly focus on protein and peptide analysis by MALDI IMS. Three different types of studies can be distinguished; diagnostic studies that compare different tissue types (e.g., tumor versus normal) to aid in the pathological diagnosis, prognostic studies that differentiate patients with long or short term survival, and drug response studies that aid in predicting a patient's response to a certain treatment.

4.1. *Protein analysis*

IMS based studies have focused on the elucidation of molecular differences in cancers by analyzing fresh frozen tissue samples from clinical specimens. In several applications using unsupervised, multiplexed and spatially resolved molecular

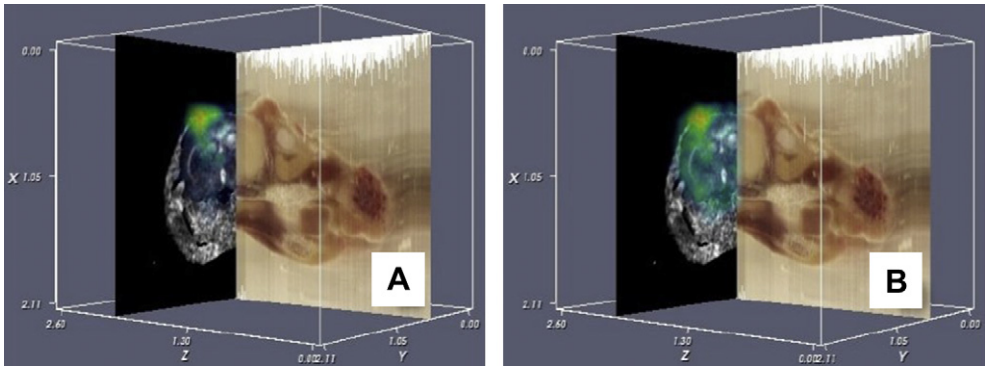

Figure 3 – Coregistration of block face optical image (brown plane) and MRI data (black and white plane) with IMS data (colored plane) from a rat brain tumor. Panel A, MS image of PEA 15 at m/z 15,035; Panel B, MS image of Fabp5 at m/z 15,076 (from Sinha et al., 2008).

data obtained by IMS, graded changes in protein distributions from tumor to adjacent normal regions of tissue were shown in clear cell renal cell carcinoma (ccRCC) (Herring et al., 2007) and malignant fibrous histiocytoma (Caldwell et al., 2006). Decreasing with distance from the tumor out to 1.5 cm in the surrounding microenvironment, these molecular changes could be observed in histologically normal appearing tissue. In another study, ccRCC samples ($n = 34$) containing both tumor and normal tissue within the same section were analyzed to assess differences in molecular distributions in tumor adjacent and tumor distant normal tissue (Oppenheimer et al., 2010). Statistical analysis revealed proteins that were under expressed in the tumor as well as the tumor adjacent normal tissue compared to the tumor distant normal tissue, again with the nearby microenvironment resembling the molecular characteristics of the tumor. Some of these proteins, for example, were identified as proteins from the mitochondrial electron transports system; cytochrome c (*m/z* 12,272), NADH-ubiquinone oxidoreductased MLRQ subunit (*m/z* 9368) and five cytochrome c oxidase polypeptides: subunit 5b (*m/z* 10,611); subunit 6C (*m/z* 8577); subunit 7A2 (*m/z* 6720); subunit 7C (*m/z* 5354) and subunit 8A (*m/z* 4890). Although the decreased expression of these proteins has previously been reported in ccRCC samples, they were not reported in adjacent histologically normal appearing tissue.

A major field of interest in cancer research involves the search for more effective diagnostic markers to differentiate between cancer and normal and moreover between different cancer subtypes and grades. However, of growing interest is the discovery of molecular markers that predict patient outcome and that distinguish between treatment responders and non-responders. Investigators seek better prognostic and treatment response markers in order to tailor treatment most beneficial for an individual patient. In terms of shrinking health care budgets, this personalized analysis would inure not only to the benefit of the patient but would also help decrease health care costs through achieving better outcomes with less side effects.

In a study of non-small cell lung cancer (NSCLC), investigators subjected fresh frozen samples from 79 lung tumors and 14 normal lung tissues to IMS (Yanagisawa et al., 2003). In a training set of 42 tumor samples (including primary and metastatic lung tumors) and 8 normal samples, 82 spectral features were found to be significantly differentially expressed between both groups. Utilizing a class-prediction model based on selected peaks, investigators were able to correctly classify all samples in the training as well as all samples of an independent validation set (37 cancer and 6 normal samples). Discrimination of different NSCLC subtypes (adenocarcinoma, squamous cell carcinoma and large cell carcinoma) and of primary NSCLC from metastases to the lung from other body sites could also be achieved based on their proteomic patterns. Prognostic proteomic patterns were determined that predict nodal status and patient survival. Expression profiles of two proteins allowed classification of tumors with and without mediastinal lymph node metastasis with 85% and 75% accuracy in the training and validation set, respectively. Distinction between NSCLC patients with poor ($n = 25$) and good ($n = 41$) prognosis could be achieved by combining 15 peaks in a proteomic pattern ($p < 0.0001$). Two proteins (*m/z* 10,519 and *m/z* 4964) highly expressed in primary NSCLC were identified as small ubiquitin-related modifier-2 protein (SUMO-2) and thymosin-β4, respectively.

Another IMS study of gliomas was able to obtain proteomic patterns that correlate with tumor histology and independently predict patient survival (Schwartz et al., 2005). Fresh frozen non-tumor samples ($n = 19$) could be distinguished from glioma samples ($n = 108$) on average with >92% accuracy. Combining 24 protein signals enabled the differentiation of a short-term survival (STS, 52 patients, mean survival <15 months) and a long-term survival (LTS, 56 patients, mean survival >90 months) group. This proteomic pattern was shown to be an independent indicator of patient survival by a multivariate Cox proportional hazards model ($p < 0.0001$). One protein overexpressed in STS patients was identified as calcyclin (S100-A6, *m/z* 10,092). Dynein light chain 2 (*m/z* 10.262) was found to be predominant in the LTS patients. In a subgroup of the glioma patients, gliobastoma multiforme patients, those with STS (28 patients, average survival 10.9 months) were distinguished from patients with LTS (29 patients, average survival 16.8 months) utilizing two peaks. Multivariate analysis also verified this pattern to be an independent predictor of patient survival. Other proteins identified in this study include calpactin I light chain (S100-A10, *m/z* 11,073), astrocytic phosphorprotein PEA-15 (*m/z* 15,035), fatty acid-binding protein 5 (*m/z* 15,076), and tubulin-specific chaperone A (*m/z*

17,268). Calcyclin, calpactin I light chain and tubulin-specific chaperone A were found to be overexpressed in grade IV gliomas whereas astrocytic phosphoprotein PEA-15 was predominant in grades II and III gliomas compared to grade IV gliomas.

In a study of breast cancer patients IMS, was shown to be a beneficial new tool in HER2 receptor classification (Rauser et al., 2010). Fresh frozen samples from 48 patients (training set = 30 and validation set = 18) were analyzed to predict the HER2 receptor status. Immunohistochemistry (IHC) and fluorescence *in situ* hybridization were used to evaluate the HER2 receptor status in the training set (HER2 positive, $n = 15$ and HER2 negative, $n = 15$) whereas the validation set (HER2 positive, $n = 6$ and HER2 negative, $n = 12$) was evaluated by IHC only. Utilizing an artificial neuronal network based model enabled prediction of the HER2 receptor status in the training set with 87% sensitivity and 93% specificity. In the independent validation set, 16 out of 18 cases were assigned correctly resulting in a sensitivity and specificity of 83% and 92%, respectively. Among the differentially expressed features, *m/z* 8404 that was overexpressed in HER2 positive samples was identified as cysteine-rich intestinal protein 1 (CRIP1). This finding is in agreement with previous reports using mRNA measurements that describe the co-expression of CRIP1 and HER2 (Mackay et al., 2003; Wilson et al., 2002).

Two other studies in the field of breast cancer research reported the identification of proteomic markers that predict treatment response in breast cancer. Samples from breast cancer patients receiving a neoadjuvant therapeutic treatment regime with paclitaxel and radiation were analyzed by histology-directed profiling and gene expression profiling (Bauer et al., 2010). From a total of 38 patients enrolled in this study, fresh frozen samples from 19 patients were available to perform IMS analysis. After treatment, 6 patients showed a pathological complete response and 13 were determined as non-responders due to presence of residual disease. Three highly overexpressed (>30-fold) features (*m/z* 3371, *m/z* 3442 and *m/z* 3485) and four features of lower expression (*m/z* 5667, *m/z* 6955, *m/z* 7007 and *m/z* 15,348) were revealed in the responder group by spectral comparison between tumor regions from both groups. As previously identified by other research groups, the three overexpressed features represent defensins (*m/z* 3371, α-DEFA1; *m/z* 3442, α-DEFA2 and *m/z* 3485, α-DEFA3). These cytotoxic peptides are primarily known to be abundant in neutrophils. IHC was performed to elucidate the source of DEFA expression and obviate a false positive result due to blood contamination of the samples. IHC results verified that besides infiltrating neutrophils, the tumor cells showed a positive staining for DEFA in patients with a pathological complete response whereas non-responders exhibited little or no staining of the tumor cells. DEFA was not found to be overexpressed in the gene expression profiling studies that only revealed genes from immune response categories to be differentially expressed. These results highlight the independent value of proteomic-based approaches and its importance in discovery of protein differences at the posttranslational level that cannot be identified at the genomic level.

An earlier study of mammary tumors in mouse mammary tumor virus/HER2 transgenic mice was able to predict treatment response to a small molecule inhibitor of the epidermal growth factor receptor tyrosine kinase (elortinib) and/or a HER2 blocking antibody (trastuzumab) by assessing early proteomic changes directly in the tumor by IMS (Reyzer et al., 2004). Fresh frozen tumor sections at various time points after drug administration were compared to sections from untreated mice. Time- and dose-dependent related proteomic changes were observed. Elortinib treatment induced a decrease in thymosin beta-4 (*m/z* 4965) as well as ubiquitin (*m/z* 8565) and an increase of a fragment of E-cadherin binding protein (*m/z* 4794) in tumor sections when compared to tumors from untreated mice. Even bigger changes in thymosin beta-4 and the fragment of E-cadherin binding protein were noticed when a combinational treatment with both drugs was administered. This combinational treatment resulted in an additional proteomic change not observed in the single dosed tumors; a calmodulin fragment (*m/z* 8719) was found to be increased considerably. Additional proteins found to be upregulated in tumors treated with both drugs include ubiquitin, acyl-CoA binding protein, calgizzarin, histone H3 and histone H4. Spatial distribution studies of elortinib obtained directly from tissue sections by IMS also correlated with these proteomic changes, thus emphasizing the strength and versatility of IMS.

Studies of prostate cancer have utilized IMS to aid in the diagnosis of this highly prevalent disease and to discover proteins relevant to the underlying biology (Cazares et al., 2009; Schwamborn et al., 2007). In one study, investigators compared 31 fresh frozen prostate cancer and 41 normal prostate biopsies with the aim to identify peptides differentially expressed between both groups (Cazares et al., 2009). Two peptides (*m/z* 4027 and *m/z* 4355) showed significant over expression in cancer samples whereas *m/z* 4274 was predominant in benign areas. For statistical analyses, the sample set was divided in a discovery set (cancer, $n = 11$; normal, $n = 10$) and an independent validation set (cancer, $n = 23$; normal, $n = 31$). A correct classification of 85% and 81% in the discovery set and validation set, respectively, was achieved by combining the three peptides in a genetic algorithm based model. The peptide at *m/z* 4355, overexpressed in cancer tissue, was identified as a fragment of mitogen-activated protein kinase/extracellular signal-regulated kinase kinase kinase 2 (MEKK2). Expression of this fragment could be shown to decrease with increasing Gleason grade and a significant reduction could be observed between pathological stage pT2 and pT3b. MEKK2 over expression could further be validated by Western blot analysis and IHC, both of which found MEKK2 overexpressed in prostate cancer tissue and prostate cancer cell lines.

In a similar study of ovarian cancer, fresh frozen ovarian cancer tissue samples ($n = 25$) were analyzed in comparison to benign ovarian tumors ($n = 23$) (Lemaire et al., 2007). A putative marker for ovarian cancer was detected at *m/z* 9744 with a prevalence of 80%. This feature was identified as a fragment of the 11S proteasome activator complex, Reg-alpha (*m/z* 9744). Validation of IMS results was performed by Western blot analysis as well as IHC. The Western blot showed a detection of the complete protein (28 kDa) in 6 of 9 carcinoma samples whereas 3 out of 16 benign tumors showed a slightly positive result. The latter revealed distinct and diagnosis dependent localization within cellular compartments with

cytoplasmatic localization of Reg-alpha in carcinomas and no cytoplasmatic but nuclear staining in 76.9% of benign tumors.

Other studies of oral squamous cell carcinoma (Patel et al., 2009), tumor interfaces in ovarian cancer (Kang et al., 2010), meningioma progression (Agar et al., 2010) and classical Hodgkin lymphoma (Schwamborn et al., 2010) also show the capabilities of IMS in these types of applications.

4.2. *Peptide analysis*

The emerging capability of the analysis of FFPE tissue specimens by IMS is an important advance of this technology. The vast majority of clinical samples stored worldwide are formalin preserved and embedded in paraffin (Wisztorski et al., 2010), many with related patient data and outcome. Mining this invaluable source of information for a wide variety of cancers promises to give new insights in cancer research. Analysis of FFPE tissue is attained by combining heat induced antigen retrieval techniques and enzymatic sample digestion (Gustafsson et al., 2010; Ronci et al., 2008; Xu et al., 2008). Even though only partial reversal of formalin induced modifications are achieved, initial studies using IMS have substantiated the capability and the potential of this approach (Groseclose et al., 2008). Tryptic digestion has also allowed high molecular weight proteins to be analyzed.

A study of FFPE tissue microarray (TMA) samples from NSCLC tissues established IMS technology as a high-throughput platform for the classification of subtypes of NSCLC (Groseclose et al., 2008). In this work, the TMA contained 22 squamous cell carcinoma cores from 14 different patients and 18 adenocarcinoma cores from 12 different patients. Spectra generated from duplicate samples were highly reproducible with no statistically significant differences observed in peak intensities between duplicates as calculated using a *t*-test and minimum 1.6-fold intensity difference comparison for the 200 most intense signals. Combing 73 peaks in a support vector machine algorithm based model enabled the correct classification of all patients. Numerous peptides from approximately 50 proteins could be identified directly from the TMA by MALDI MS/MS analysis. For example, three tryptic peptides (*m*/*z* 987.60; *m*/*z* 1163.62 and *m*/*z* 1905.99) that were almost exclusively expressed in squamous cell carcinomas were identified as originating from heat shock protein beta-1. These three peptides exhibited a similar distribution across the TMA, thus further verifying their derivation from the same protein. Another peptide (*m*/*z* 1410.70), identified as a tryptic peptide from keratin type II cytoskeletal 5, showed a selective distribution in a subset of the squamous cell carcinoma samples.

Two recent studies on FFPE tissue samples from pancreatic adenocarcinoma samples using MALDI ion mobility MS also showed that it is possible to identify proteins directly from FFPE tissue sections through the identification of tryptic peptides that might aid in the diagnosis (Djidja et al., 2010, 2009). MALDI ion mobility MS allows for an additional level of separation based on the analyte's size and charge resulting in the possible separation of analytes with the same nominal molecular weight and therefore the removal of the interfering signals.

Unpublished work from our group on a TMA constructed from normal FFPE tissue samples from 12 different organ sites, 30 different tumor samples and 16 different cell lines not only showed the reproducibility of on-tissue tryptic digestion but also revealed unique features for several organ sites and tumors (Figure 4). For example, squamous cell carcinoma samples of the lung and skin showed a feature at *m*/*z* 1891.3 that could not be detected in any of the other cores. This result was consistent over time when comparing serial sections of the TMA analyzed on four different days (0, 17, 20 and 24). Another feature at *m*/*z* 1829.2 was present at relatively high levels in the hippocampus and was identified by tandem MS

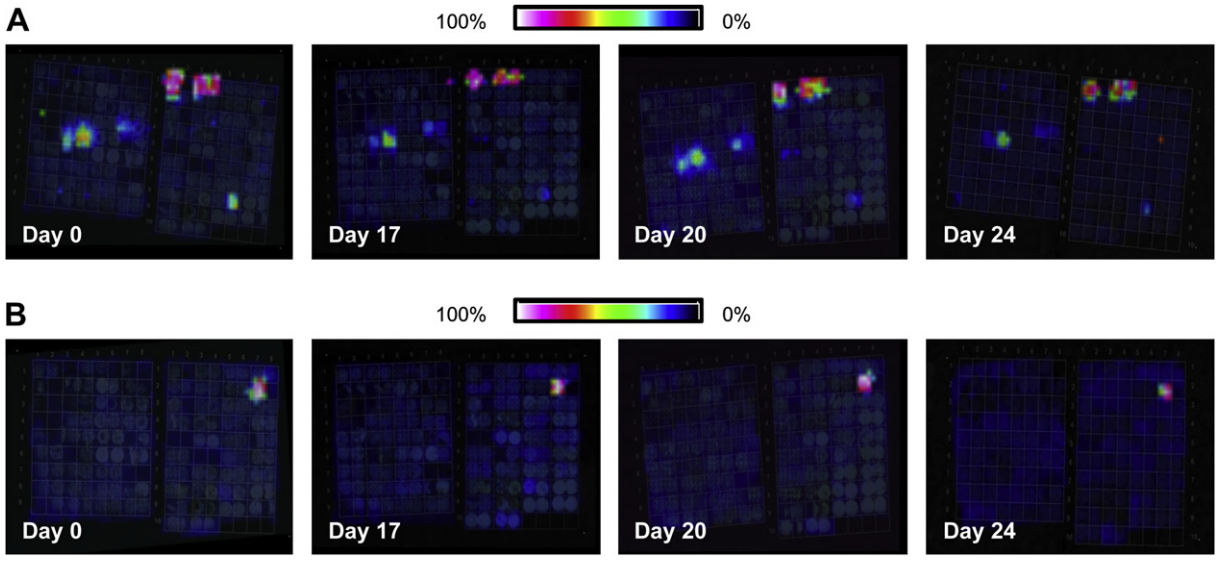

Figure 4 – Reproducibility of on-tissue tryptic digestion from a TMA comprising samples from multiple different organ sites and cancers. A: A feature at *m*/*z* 1891.3 was found only in squamous cell carcinoma samples of the lung (left column) and skin (right column). B: A feature at *m*/*z* 1829.2 was present only in the hippocampus. Both features were reproducible when comparing serial sections that were analyzed on four different days.

directly from the tissue as a tryptic peptide of tubulin beta-4 chain.

4.3. *Lipids and drugs*

IMS analysis of tissue sections also allows the direct analysis of small molecules including lipids and drugs from fresh frozen tissue sections. Sample pretreatment is slightly different for these analytes with the most important aspect of avoiding tissue washing steps in order to preserve analyte levels.

Alterations in lipid levels have been described in many human diseases including cancer (Wenk, 2005). With growing interest, IMS has been utilized to evaluate lipid changes in a spatially resolved manner, e.g., revealing regional differences in concentrations for specific molecular lipid species such as cardiolipins in different rat organ sections (Wang et al., 2007) or phospholipid distribution during mouse embryo implantation (Burnum et al., 2009). Cancer related lipid changes were discovered in a study of 78 matched ccRCC samples (S. Puolitaival and R.M. Caprioli, unpublished results). Tumor regions showed a higher abundance of linoleic acid containing phospholipids whereas normal regions contained more sphingomyelins.

IMS was employed to assess the distribution of drugs within tissue sections, an important aspect in drug discovery studies to understand drug metabolism and drug induced changes to proteins and other metabolites (Cornett et al., 2008; Reyzer et al., 2003). The analysis is typically performed by tandem mass spectrometry (MS/MS) in a high throughput manner by single or multiple reaction monitoring (Wagner et al., 2008). Selected fragments of the target analyte, chosen based on their high abundance, are monitored. Initial studies have shown the possibility to detect not only the distribution of the drug itself but simultaneously the distribution of its individual metabolites within whole-body tissue sections in animal studies (Khatib-Shahidi et al., 2006).

In a recently published study, investigators measured the localization of oxaliplatin and its derivates in heated intraoperative chemotherapy-like treated rat kidneys using IMS (Bouslimani et al., 2010). From 15 μm thick tissue sections, oxaliplatin was detectable down to 0.23 ± 0.05 mg of total oxaliplatin per gram of tissue. Oxaliplatin and its derivates were localized by IMS in the kidney cortex whereas in the medulla little or no drug penetration was observed. In another study, to visualize the distribution of vinblastine within different organs, investigators imaged rat whole-body sections by IMS (Trim et al., 2008). A higher concentration of vinblastine (precursor ion *m*/*z* 811.4) and its fragments (e.g., *m*/*z* 793) was found within the liver, kidney and tissue surrounding the gastrointestinal tract. Similarly, the distribution of a small-molecule epidermal growth factor receptor inhibitor (erlotinib) and its metabolites was analyzed by IMS in tissue sections from rat liver, spleen and muscle (Signor et al., 2007). After oral administration of the drug, highest concentrations of the drug and its major metabolite were found in liver sections. Comparing direct quantitative analysis of the drug by MALDI MS with standard liquid chromatography tandem MS analysis (LC-MS/MS) on tissue homogenates resulted in similar ratios of total ion intensities from liver and spleen.

5. Perspective

MALDI imaging mass spectrometry is an effective new technology for the discovery of molecular signatures of disease including cancer. Its strengths lie in its independence from target-specific reagents such as antibodies, its capability of direct identification of analytes, and its capability to analyze multiple analytes simultaneously. IMS has become a platform technology not only for the analysis of intact proteins and peptides but also for small molecules such as drugs and lipids. As instruments and protocols further develop and mature, the analysis of more low abundance proteins and subcellular compartments will be within reach. Initial progress has already been achieved, for example, in the analysis of membrane bound proteins that has been enabled through special sample pretreatment protocols or in the analysis of FFPE samples through *in situ* tryptic digestion.

Many studies have proven the feasibility and strength of this technology especially in a discovery setting. However, more comprehensive studies involving many hundreds of samples are needed to achieve the translation of this technology from bench to bedside. Validation studies are key in establishing IMS as an effective and robust tool in a clinical setting, especially in support of personalized medicine. Protein signatures obtained directly from patient biopsies by IMS will play a key role in the future, not only in disease diagnosis but also prognosis and evaluation of therapeutic response.

Acknowledgement

This work was supported by NIH/NIGMS Grant 5R01GM058008-11, DOD Grant W81XWH-05-1-0179, NIH/NCI Grant 5P30 CA068485-13 and National Foundation for Cancer Research. The authors would like to thank P.J. Wild for providing the TMA and T.K. Sinha for 3D images.

REFERENCES

Aebersold, R., Mann, M., 2003. Mass spectrometry-based proteomics. Nature 422, 198–207.

Aerni, H.R., Cornett, D.S., Caprioli, R.M., 2006. Automated acoustic matrix deposition for MALDI sample preparation. Anal. Chem. 78, 827–834.

Agar, N.Y., Malcolm, J.G., Mohan, V., Yang, H.W., Johnson, M.D., Tannenbaum, A., Agar, J.N., Black, P.M., 2010. Imaging of meningioma progression by matrix-assisted laser desorption ionization time-of-flight mass spectrometry. Anal. Chem.

Andersson, M., Groseclose, M.R., Deutch, A.Y., Caprioli, R.M., 2008. Imaging mass spectrometry of proteins and peptides: 3D volume reconstruction. Nat. Methods 5, 101–108.

Bauer, J.A., Chakravarthy, A.B., Rosenbluth, J.M., Mi, D., Seeley, E.H., De Matos Granja-Ingram, N., Olivares, M.G., Kelley, M.C., Mayer, I.A., Meszoely, I.M., Means-Powell, J.A., Johnson, K.N., Tsai, C.J., Ayers, G.D., Sanders, M.E., Schneider, R.J., Formenti, S.C., Caprioli, R.M., Pietenpol, J.A., 2010. Identification of markers of taxane sensitivity using proteomic and genomic analyses of breast tumors from

patients receiving neoadjuvant paclitaxel and radiation. Clin. Cancer Res. 16, 681–690.
Becker, K.F., Schott, C., Hipp, S., Metzger, V., Porschewski, P., Beck, R., Nahrig, J., Becker, I., Hofler, H., 2007. Quantitative protein analysis from formalin-fixed tissues: implications for translational clinical research and nanoscale molecular diagnosis. J. Pathol. 211, 370–378.
Bouslimani, A., Bec, N., Glueckmann, M., Hirtz, C., Larroque, C., 2010. Matrix-assisted laser desorption/ionization imaging mass spectrometry of oxaliplatin derivatives in heated intraoperative chemotherapy (HIPEC)-like treated rat kidney. Rapid Commun. Mass Spectrom. 24, 415–421.
Burnum, K.E., Cornett, D.S., Puolitaival, S.M., Milne, S.B., Myers, D.S., Tranguch, S., Brown, H.A., Dey, S.K., Caprioli, R.M., 2009. Spatial and temporal alterations of phospholipids determined by mass spectrometry during mouse embryo implantation. J. Lipid Res. 50, 2290–2298.
Caldwell, R.L., Gonzalez, A., Oppenheimer, S.R., Schwartz, H.S., Caprioli, R.M., 2006. Molecular assessment of the tumor protein microenvironment using imaging mass spectrometry. Cancer Genomics Proteomics 3, 279–288.
Caprioli, R.M., Farmer, T.B., Gile, J., 1997. Molecular imaging of biological samples: localization of peptides and proteins using MALDI-TOF MS. Anal. Chem. 69, 4751–4760.
Cazares, L.H., Troyer, D., Mendrinos, S., Lance, R.A., Nyalwidhe, J.O., Beydoun, H.A., Clements, M.A., Drake, R.R., Semmes, O.J., 2009. Imaging mass spectrometry of a specific fragment of mitogen-activated protein kinase/extracellular signal-regulated kinase kinase kinase 2 discriminates cancer from uninvolved prostate tissue. Clin. Cancer Res. 15, 5541–5551.
Celis, J.E., Gromov, P., 2003. Proteomics in translational cancer research: toward an integrated approach. Cancer Cell 3, 9–15.
Chaurand, P., Caprioli, R.M., 2002. Direct profiling and imaging of peptides and proteins from mammalian cells and tissue sections by mass spectrometry. Electrophoresis 23, 3125–3135.
Chaurand, P., Schwartz, S.A., Billheimer, D., Xu, B.J., Crecelius, A., Caprioli, R.M., 2004. Integrating histology and imaging mass spectrometry. Anal. Chem. 76, 1145–1155.
Chaurand, P., Schwartz, S.A., Caprioli, R.M., 2002. Imaging mass spectrometry: a new tool to investigate the spatial organization of peptides and proteins in mammalian tissue sections. Curr. Opin. Chem. Biol. 6, 676–681.
Chaurand, P., Schwartz, S.A., Reyzer, M.L., Caprioli, R.M., 2005. Imaging mass spectrometry: principles and potentials. Toxicol. Pathol. 33, 92–101.
Chen, E.I., Yates 3rd, J.R., 2007. Cancer proteomics by quantitative shotgun proteomics. Mol. Oncol. 1, 144–159.
Cornett, D.S., Frappier, S.L., Caprioli, R.M., 2008. MALDI-FTICR imaging mass spectrometry of drugs and metabolites in tissue. Anal. Chem. 80, 5648–5653.
Cornett, D.S., Mobley, J.A., Dias, E.C., Andersson, M., Arteaga, C.L., Sanders, M.E., Caprioli, R.M., 2006. A novel histology-directed strategy for MALDI-MS tissue profiling that improves throughput and cellular specificity in human breast cancer. Mol. Cell. Proteomics 5, 1975–1983.
Cornett, D.S., Reyzer, M.L., Chaurand, P., Caprioli, R.M., 2007. MALDI imaging mass spectrometry: molecular snapshots of biochemical systems. Nat. Methods 4, 828–833.
Crecelius, A.C., Cornett, D.S., Caprioli, R.M., Williams, B., Dawant, B.M., Bodenheimer, B., 2005. Three-dimensional visualization of protein expression in mouse brain structures using imaging mass spectrometry. J. Am. Soc. Mass Spectrom. 16, 1093–1099.
Deininger, S.O., Ebert, M.P., Futterer, A., Gerhard, M., Rocken, C., 2008. MALDI imaging combined with hierarchical clustering as a new tool for the interpretation of complex human cancers. J. Proteome Res. 7, 5230–5236.
Djidja, M.C., Claude, E., Snel, M.F., Francese, S., Scriven, P., Carolan, V., Clench, M.R., 2010. Novel molecular tumour classification using MALDI-mass spectrometry imaging of tissue micro-array. Anal. Bioanal. Chem.
Djidja, M.C., Claude, E., Snel, M.F., Scriven, P., Francese, S., Carolan, V., Clench, M.R., 2009. MALDI-ion mobility separation-mass spectrometry imaging of glucose-regulated protein 78 kDa (Grp78) in human formalin-fixed, paraffin-embedded pancreatic adenocarcinoma tissue sections. J. Proteome Res. 8, 4876–4884.
Grey, A.C., Chaurand, P., Caprioli, R.M., Schey, K.L., 2009. MALDI imaging mass spectrometry of integral membrane proteins from ocular lens and retinal tissue. J. Proteome Res. 8, 3278–3283.
Groseclose, M.R., Massion, P.P., Chaurand, P., Caprioli, R.M., 2008. High-throughput proteomic analysis of formalin-fixed paraffin-embedded tissue microarrays using MALDI imaging mass spectrometry. Proteomics 8, 3715–3724.
Gustafsson, J.O., Oehler, M.K., McColl, S.R., Hoffmann, P., 2010. Citric acid antigen retrieval (CAAR) for tryptic peptide imaging directly on archived formalin-fixed paraffin-embedded tissue. J. Proteome Res. 9, 4315–4328.
Hankin, J.A., Barkley, R.M., Murphy, R.C., 2007. Sublimation as a method of matrix application for mass spectrometric imaging. J. Am. Soc. Mass Spectrom. 18, 1646–1652.
Hanselmann, M., Köthe, U., Kirchner, M., Renard, B.Y., Amstalden, E.R., Glunde, K., Heeren, R.M.A., Hamprecht, F.A., 2009. Toward digital staining using imaging mass spectrometry and random forests. J. Proteome Res. 8, 3558–3567.
Harvey, D.J., Naven, T.J., Kuster, B., Bateman, R.H., Green, M.R., Critchley, G., 1995. Comparison of fragmentation modes for the structural determination of complex oligosaccharides ionized by matrix-assisted laser desorption/ionization mass spectrometry. Rapid Commun. Mass Spectrom. 9, 1556–1561.
Herring, K.D., Oppenheimer, S.R., Caprioli, R.M., 2007. Direct tissue analysis by matrix-assisted laser desorption ionization mass spectrometry: application to kidney biology. Semin. Nephrol. 27, 597–608.
Kang, S., Shim, H.S., Lee, J.S., Kim, D.S., Kim, H.Y., Hong, S.H., Kim, P.S., Yoon, J.H., Cho, N.H., 2010. Molecular proteomics imaging of tumor interfaces by mass spectrometry. J. Proteome Res. 9, 1157–1164.
Karas, M., Hillenkamp, F., 1988. Laser desorption ionization of proteins with molecular masses exceeding 10,000 daltons. Anal. Chem. 60, 2299–2301.
Khatib-Shahidi, S., Andersson, M., Herman, J.L., Gillespie, T.A., Caprioli, R.M., 2006. Direct molecular analysis of whole-body animal tissue sections by imaging MALDI mass spectrometry. Anal. Chem. 78, 6448–6456.
Krieg, R.C., Gaisa, N.T., Paweletz, C.P., Knuechel, R., 2005. Proteomic analysis of human bladder tissue using SELDI approach following microdissection techniques. Methods Mol. Biol. 293, 255–267.
Krieg, R.C., Paweletz, C.P., Liotta, L.A., Petricoin 3rd, E.F., 2002. Clinical proteomics for cancer biomarker discovery and therapeutic targeting. Technol. Cancer Res. Treat. 1, 263–272.
Kruse, R., Sweedler, J.V., 2003. Spatial profiling invertebrate ganglia using MALDI MS. J. Am. Soc. Mass Spectrom. 14, 752–759.
Lemaire, R., Ait Menguellet, S., Stauber, J., Marchaudon, V., Lucot, J.-P., Collinet, P., Farine, M.-O., Vinatier, D., Day, R., Ducoroy, P., Salzet, M., Fournier, I., 2007. Specific MALDI imaging and profiling for biomarker hunting and validation: fragment of the 11S proteasome activator complex, reg alpha

fragment, is a new potential ovary cancer biomarker. J. Proteome Res. 6, 4127–4134.
Mackay, A., Jones, C., Dexter, T., Silva, R.L., Bulmer, K., Jones, A., Simpson, P., Harris, R.A., Jat, P.S., Neville, A.M., Reis, L.F., Lakhani, S.R., O'Hare, M.J., 2003. cDNA microarray analysis of genes associated with ERBB2 (HER2/neu) over expression in human mammary luminal epithelial cells. Oncogene 22, 2680–2688.
Mueller, C., Liotta, L.A., Espina, V., 2010. Reverse phase protein microarrays advance to use in clinical trials. Mol. Oncol 4 (6), 461–481.
Oppenheimer, S.R., Mi, D., Sanders, M., Caprioli, R.M., 2010. A molecular analysis of tumor margins by MALDI mass spectrometry in renal carcinoma. J. Proteome Res..
Patel, S.A., Barnes, A., Loftus, N., Martin, R., Sloan, P., Thakker, N., Goodacre, R., 2009. Imaging mass spectrometry using chemical inkjet printing reveals differential protein expression in human oral squamous cell carcinoma. Analyst 134, 301–307.
Puolitaival, S.M., Burnum, K.E., Cornett, D.S., Caprioli, R.M., 2008. Solvent-free matrix dry-coating for MALDI imaging of phospholipids. J. Am. Soc. Mass Spectrom. 19, 882–886.
Rauser, S., Marquardt, C., Balluff, B., Deininger, S.O., Albers, C., Belau, E., Hartmer, R., Suckau, D., Specht, K., Ebert, M.P., Schmitt, M., Aubele, M., Hofler, H., Walch, A., 2010. Classification of HER2 receptor status in breast cancer tissues by MALDI imaging mass spectrometry. J. Proteome Res.
Reyzer, M.L., Caldwell, R.L., Dugger, T.C., Forbes, J.T., Ritter, C.A., Guix, M., Arteaga, C.L., Caprioli, R.M., 2004. Early changes in protein expression detected by mass spectrometry predict tumor response to molecular therapeutics. Cancer Res. 64, 9093–9100.
Reyzer, M.L., Hsieh, Y., Ng, K., Korfmacher, W.A., Caprioli, R.M., 2003. Direct analysis of drug candidates in tissue by matrix-assisted laser desorption/ionization mass spectrometry. J. Mass Spectrom. 38, 1081–1092.
Ronci, M., Bonanno, E., Colantoni, A., Pieroni, L., Di Ilio, C., Spagnoli, L.G., Federici, G., Urbani, A., 2008. Protein unlocking procedures of formalin-fixed paraffin-embedded tissues: application to MALDI-TOF imaging MS investigations. Proteomics 8, 3702–3714.
Schiller, J., Suss, R., Arnhold, J., Fuchs, B., Lessig, J., Muller, M., Petkovic, M., Spalteholz, H., Zschornig, O., Arnold, K., 2004. Matrix-assisted laser desorption and ionization time-of-flight (MALDI-TOF) mass spectrometry in lipid and phospholipid research. Prog. Lipid Res. 43, 449–488.
Schwamborn, K., Krieg, R., Jirak, P., Ott, G., Knüchel, R., Rosenwald, A., Wellmann, A., 2010. Application of MALDI imaging for the diagnosis of classical hodgkin lymphoma. J. Cancer Res. Clin. Oncol.
Schwamborn, K., Krieg, R.C., Reska, M., Jakse, G., Knuechel, R., Wellmann, A., 2007. Identifying prostate carcinoma by MALDI-Imaging. Int. J. Mol. Med. 20, 155–159.
Schwartz, S.A., Reyzer, M.L., Caprioli, R.M., 2003. Direct tissue analysis using matrix-assisted laser desorption/ionization mass spectrometry: practical aspects of sample preparation. J. Mass Spectrom. 38, 699–708.
Schwartz, S.A., Weil, R.J., Thompson, R.C., Shyr, Y., Moore, J.H., Toms, S.A., Johnson, M.D., Caprioli, R.M., 2005. Proteomic-based prognosis of brain tumor patients using direct-tissue matrix-assisted laser desorption ionization mass spectrometry. Cancer Res. 65, 7674–7681.
Seeley, E.H., Caprioli, R.M., 2008. Molecular imaging of proteins in tissues by mass spectrometry. Proc. Natl. Acad. Sci. U.S.A. 105, 18126–18131.
Signor, L., Varesio, E., Staack, R.F., Starke, V., Richter, W.F., Hopfgartner, G., 2007. Analysis of erlotinib and its metabolites in rat tissue sections by MALDI quadrupole time-of-flight mass spectrometry. J. Mass Spectrom. 42, 900–909.
Sinha, T.K., Khatib-Shahidi, S., Yankeelov, T.E., Mapara, K., Ehtesham, M., Cornett, D.S., Dawant, B.M., Caprioli, R.M., Gore, J.C., 2008. Integrating spatially resolved three-dimensional MALDI IMS with in vivo magnetic resonance imaging. Nat. Methods 5, 57–59.
Sloane, A.J., Duff, J.L., Wilson, N.L., Gandhi, P.S., Hill, C.J., Hopwood, F.G., Smith, P.E., Thomas, M.L., Cole, R.A., Packer, N.H., Breen, E.J., Cooley, P.W., Wallace, D.B., Williams, K.L., Gooley, A.A., 2002. High throughput peptide mass fingerprinting and protein macroarray analysis using chemical printing strategies. Mol. Cell. Proteomics 1, 490–499.
Stoeckli, M., Chaurand, P., Hallahan, D.E., Caprioli, R.M., 2001. Imaging mass spectrometry: a new technology for the analysis of protein expression in mammalian tissues. Nat. Med. 7, 493–496.
Tanaka, K., Waki, H., Ido, Y., Akita, S., Yoshida, Y., Yoshida, T., Matsuo, T., 1988. Protein and polymer analyses up to *m/z* 100 000 by laser ionization time-of-flight mass spectrometry. Rapid Commun. Mass Spectrom. 2, 151–153.
Tost, J., Gut, I.G., 2006. DNA analysis by mass spectrometry-past, present and future. J. Mass Spectrom. 41, 981–995.
Trim, P.J., Henson, C.M., Avery, J.L., McEwen, A., Snel, M.F., Claude, E., Marshall, P.S., West, A., Princivalle, A.P., Clench, M.R., 2008. Matrix-assisted laser desorption/ionization-ion mobility separation-mass spectrometry imaging of vinblastine in whole body tissue sections. Anal. Chem. 80, 8628–8634.
van der Merwe, D.E., Oikonomopoulou, K., Marshall, J., Diamandis, E.P., 2007. Mass spectrometry: uncovering the cancer proteome for diagnostics. Adv. Cancer Res. 96, 23–50.
Wagner, M., Varesio, E., Hopfgartner, G., 2008. Ultra-fast quantitation of saquinavir in human plasma by matrix-assisted laser desorption/ionization and selected reaction monitoring mode detection. J. Chromatogr. B. 872, 68–76.
Walch, A., Rauser, S., Deininger, S.O., Hofler, H., 2008. MALDI imaging mass spectrometry for direct tissue analysis: a new frontier for molecular histology. Histochem. Cell Biol. 130, 421–434.
Wang, H.Y., Jackson, S.N., Woods, A.S., 2007. Direct MALDI-MS analysis of cardiolipin from rat organs sections. J. Am. Soc. Mass Spectrom. 18, 567–577.
Wenk, M.R., 2005. The emerging field of lipidomics. Nat. Rev. Drug Discov. 4, 594–610.
Wilson, K.S., Roberts, H., Leek, R., Harris, A.L., Geradts, J., 2002. Differential gene expression patterns in HER2/neu-positive and -negative breast cancer cell lines and tissues. Am. J. Pathol. 161, 1171–1185.
Wisztorski, M., Franck, J., Salzet, M., Fournier, I., 2010. MALDI direct analysis and imaging of frozen versus FFPE tissues: what strategy for which sample? Methods Mol. Biol. 656, 303–322.
Xu, H., Yang, L., Wang, W., Shi, S.R., Liu, C., Liu, Y., Fang, X., Taylor, C.R., Lee, C.S., Balgley, B.M., 2008. Antigen retrieval for proteomic characterization of formalin-fixed and paraffin-embedded tissues. J. Proteome Res. 7, 1098–1108.
Yanagisawa, K., Shyr, Y., Xu, B.J., Massion, P.P., Larsen, P.H., White, B.C., Roberts, J.R., Edgerton, M., Gonzalez, A., Nadaf, S., Moore, J.H., Caprioli, R.M., Carbone, D.P., 2003. Proteomic patterns of tumour subsets in non-small-cell lung cancer. Lancet 362, 433–439.